www.czasopisma.pan.pl PAN POLSKA AKADEMIA NAUK www.journals.pan.pl

Arch. Min. Sci. **69** (2024), 4, 633-654

Electronic version (in color) of this paper is available: http://mining.archives.pl

DOI: https://doi.org/10.24425/ams.2024.152578

DONGDONG PANG[1,2*], XI WANG[1], ZHIQIANG YIN[1], XINGANG NIU[1], PENG YANG[1], ZONGYU NI[1]

STUDY ON UPPER AND LOWER GAS DRAINAGE AND PREVENTION AND CONTROL TECHNOLOGIES IN DEEP HIGH-GAS MINES

In response to the "three highs" problem in the mining of deep high-gas mines, the rapid increase in the coal seam permeability coefficient and gradual increase in coal and gas outburst problems have made gas control more difficult. This study considered the occurrence of remote outburst coal seams in the Zhujixi Mine as the research background and performed theoretical analysis, calculations, numerical simulations, and other technical methods to analyze the gas occurrence characteristics of the 11-2 coal seam and the feasibility of using this seam as a lower protective layer for mining. The pressure relief protection range for the overlying 13-1 coal seam, to the recovery of the 11-2 coal seam, was determined. A regional anti-outburst technology was proposed for underground through-layer and parallel-layer drilling, focusing on pre-gas extraction for the protective layer. In addition, a pre-gas extraction regional anti-outburst technology combining the surface and underground mining of the protected layer is also proposed.

Gas occurrence in the 11-2 coal seam is uneven and has poor regularity, presenting high gas areas. It is significantly affected by the geological structures and shale properties of the coal seam roof and floor. The 11-2 coal seam is a stress-dominated and gas-outburst coal seam. The Zhujixi Mine presents a joint underground extraction and regional outburst prevention mode; that is, the 11-2 coal seam with a lower outburst risk is selected as the protective layer for mining first, whereas the 13-1 coal seam is protected while the gas in the protected layer is extracted. The 11-2 coal is characterized by the gas control mode of "one side, three lanes+ground drillings" to achieve multi-purpose, joint treatment, and continuous mining of one lane. The excavation face exhibits comprehensive anti-outburst measures, such as through-layer drilling pre-extraction and a coal mining face over the layer drilling pre-extraction area. During the mining period, surface drilling and a top extraction roadway are used to extract 13-1 coal-depressurized gas. By adopting joint extraction technology in the upper and lower mining areas, the residual gas content and pressure were measured at the underground excavation and mining working face. The predicted indicators did not exceed the standard levels, and no dynamic phenomena occurred. As a result of the application of the anti-outburst technology in the joint extraction area of the Zhujixi Mine, the proportion of extraction in the

[1] ANHUI UNIVERSITY OF SCIENCE AND TECHNOLOGY, SCHOOL OF MINING ENGINEERING, HUAINAN, ANHUI 232001, CHINA

[2] THE COAL MINE SAFETY MINING EQUIPMENT INNOVATION CENTER OF ANHUI PROVINCE, ANHUI UNIVERSITY OF SCIENCE AND TECHNOLOGY, HUAINAN, ANHUI 232001, CHINA

* Corresponding author: 793053508@qq.com

upper and lower mining areas was 56.7%, and the proportion of extraction in the underground mining area was 43.3%. These factors are interdependent and indispensable. The maximum height of the caving zone after mining the 11-2 coal face was 11.6 m, whereas the height of the fracture zone was 34.4-52.2 m. The 13-1 protective-layer working face is arranged on the upper part of the fracture zone or lower part of the curved subsidence zone, which can effectively increase the permeability of the 13-1 coal seam. Engineering practice has shown that the joint regional anti-outburst technology and engineering application in Zhujixi mine have achieved good results, forming a regional anti-outburst technology system for joint extraction of mines and providing a reference for the safety production of similar conditions in outburst mines.

Keywords: Gas drainage; Gas control; Deep well mining; Regional outburst prevention

Introduction

Coal is the primary source of energy in China. China is among the countries with the most serious gas disasters. The endowment of coal resources and long-term strong demand led to the rapid transfer of China's coal development to the deep at the speed of 10-25 m per year. The gas problem faced by deep coal mining is more serious. Considering the three aspects of safety, energy, and environmental protection, it is necessary to strengthen the co-mining of coal and gas in deep coal seams [1-3]. The safe and efficient mining of kilometre-deep wells faces technical problems such as high ground stress, high gas, and high and low temperature [4-5]. The task of preventing gas disasters is still very arduous. With the increase of mining depth, the deep coal seam is in the complex environment of "three highs", and the gas problem faced by the development of coal resources will be more serious [6]. When the coal seam is mined more and more downward, the coupling relationship between gas pressure and content becomes increasingly unclear, and the dynamic phenomenon dominated by in-situ stress will become increasingly obvious, and gradually develop into the key to causing outburst. Especially in deep roadway mining, the surrounding rock characteristics of the stope have changed dramatically, the underground working environment has changed dramatically, and coal and gas outburst still occurs when the gas content and gas pressure do not exceed the critical value [7], resulting in hidden dangers in safety production. Coal and gas outburst is a common dynamic disaster in underground coal mining, characterized by the continuous rupture and instability of the coal rock system in a very short time, accompanied by the violent spraying of high-pressure gas into the mining space, causing mining disasters such as explosion and damage to the mining space. How to deal with more frequent and complex outburst disasters in deep coal layers is a major challenge facing coal mine safety production [8]. Due to technological and spatial limitations, it is impossible to monitor the development and propagation process of coal and gas outbursts in real time. Many scholars use physical and numerical simulation methods to study the mechanism of coal and gas outbursts and obtain relevant data [9-10], providing theoretical support for the prevention and control of coal and gas outburst disasters in mines. With the continuous improvement of coal mining depth, the permeability of coal seams will become worse and worse. This is a very unfavorable condition for the prevention and control of gas disasters, and it also has certain limitations for the safety production of coal mines. Coal seam strengthening is an effective way to improve gas drainage, and the key is to change the coal structure [11-13].

Protective layer mining technology can increase the micro-cracks of the coal body and release in-situ stress, to improve the permeability of the coal seam, produce a "pressure relief and flow increase effect" and realize effective gas drainage [14-17]. For outburst coal seam without a protective layer, can reduce the external stress of the coal seam and change the physical and mechanical properties of coal, A variety of anti-reflection technologies of the coal seam have

been tested and applied, including large-diameter drilling, cross drilling, and deep hole, dredging blasting, hydraulic anti-reflection, and gas explosion anti-reflection. Taking the mining coal seam of Zhujixi mine as the research object, this paper investigates the occurrence and gas geological data of the 11-2 Coal Seam in Zhujixi mine, studies and analyses the gas storage characteristics and outburst risk degree of 11-2 Coal Seam, and explores the key technology of long-distance coal seam group up and down combined pumping and outburst prevention, which lays a foundation for the continuity of mine wat control and mining, and has guiding significance for mine safety production.

1. Analysis of coal seam gas occurrence characteristics

1.1. Coal seam gas occurrence

The sedimentary environment of the coal-bearing rock series in the mine is stable, and the thickness of each coal-bearing section, coal seam spacing, and coal seam thickness are relatively stable. The spacing between 11-2 and 13-1 coal seams is 67.08~86.30 m, with an average spacing of 74.36 m. Coal seam 13-1 is mainly distributed in the deep part of line 35 to line 37, with a thickness of 2.18~5.29 M and an average of 4.0 m. It is dominated by thick coal. The coal seam minability index is 1.00, and the coefficient of variation is 24%. It is a stable coal seam. The roof is mudstone, a few points are sandstone, and the floor is mudstone and carbonaceous mudstone. The lower part of the coal seam 13-1 is 74.36 m away from coal seam 11-2.

Coal seam 11-2: the thickness is 0.77~1.80 m, with an average of 1.55 m, the coal seam minability index is 1.00, and the coefficient of variation is 19%. The roof is mainly composed of mudstone and siltstone, with light grey fine sandstone in the middle and lower parts, and interbedded with siltstone and fine sandstone in some parts; The floor is dominated by mudstone, and the middle and lower parts are siltstone and fine sandstone. The mudstone of the roof and floor belongs to soft rock ~ semi-hard rock, the siltstone belongs to semi-hard rock, and the fine sandstone belongs to hard rock. During the development preparation period, the measured maximum gas pressure of coal seam 11-2 in the first mining of the mine was 1.2 MPa, and the gas content was 2.23~8.63 m^3/t; The maximum gas pressure of 13-1 coal seam is 1.36 MPa and the gas content is 3.93~8.48 m^3/t, as shown in Fig. 1.

1.2. Influencing factors of coal seam gas occurrence

The buried depth of coal seam is the main factor affecting gas content [18-20]. With the increase of coal seam buried depth, the overlying strata make the coal seam and roadway surrounding rock from loose to dense under the action of self-weight pressure. The average buried depth of coal seam 11-2 is more than 900 m, the overlying thickness is 340~600 m, and the tertiary and quaternary new strata are covered. The linear regression relationship between geological exploration gas content and buried depth is shown in Fig. 2.

According to the regression analysis, there is a positive correlation between the two on the whole, that is, the gas content in coal seam increases with the increase of buried depth, but the increasing trend is not obvious, and the correlation coefficient is only 0.1421, indicating that the gas occurrence in coal seam 11-2 is less affected by buried depth.

Comprehensive Column and Gas Presence Diagram of Drilling in the First Mining Area				
Columnar	Layer thickness (m)	Accumulated layer thickness (m)	lithology	remarks
	3.90	3.90	13-1 coal	Maximum gas pressure 1.36MPa, gas content 3.93-8.48m3/t
	7.50	11.40	mudstone	
	0.40	11.80	Charcoal mudstone	
	8.60	20.40	mudstone	
	6.60	27.00	Siltstone	
	10.90	37.90	mudstone	
	9.10	47.00	fine sandstone	
	4.00	51.00	mudstone	
	1.20	52.30	fine sandstone	
	4.30	56.50	mudstone	
	1.60	58.10	Siltstone	
	5.10	63.20	mudstone	
	6.35	63.55	11-4 coal	
	2.90	66.45	mudstone	
	0.35	66.80	11-3 coal	
	5.20	72.00	mudstone	
	1.60	73.60	11-2 coal	maximum gas pressure is 1.2MPa, gas content is 2.23-8.63m3/t
	6.00	79.60	mudstone	

Fig. 1. Comprehensive Column and Gas Presence Diagram of Drilling in the First Mining Area

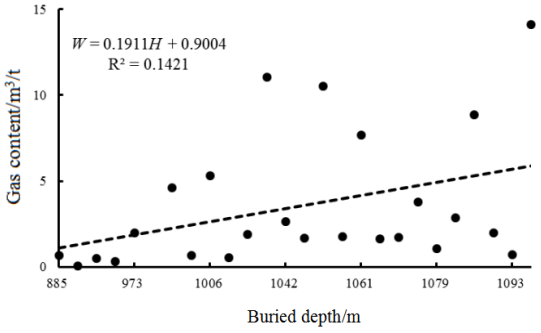

Fig. 2. 11-2 Linear regression relationship diagram between geological exploration gas content and buried depth

The influence of geological structure on gas storage is influenced by the structural form. For example, closed geological structures such as compression and torsion faults are favorable for gas storage, so the gas content is significant. Open geological structures such as tensile faults can accelerate gas release and have low gas content. Under normal conditions, the axis and inclined end of the gentle fold can promote the storage of gas, and the gas content is significant. For example, the gas content in the axis of the anticline is greater than that in the two wings.

If the tensile fractures in the axis are developed and denuded, the gas will easily escape, which is unfavorable for the storage of gas. In addition, the axial stress of the syncline is mainly compression, and the fracture is not developed, which makes it easy to produce gas enrichment, and its content will also become higher [21-23].

The measured gas content near the structure of 11501 working face in the Zhujixi mine is relatively large, which is 5.96~8.38 m^3/t. The measured gas content of the 11051 working face is affected by the structure. In the area near the fault and fold, the gas content is generally 5.90~8.39 m^3/t, in the area without geological structure, the gas content is 3.71~5.21 m^3/t, and the gas content in the geological structure zone is relatively high.

1.3. Analysis of gas occurrence law

Through drilling and statistical analysis of gas content in the 11501 working faces of the 11-2 coal seam, it was found that there were 4 groups with gas content $W \geq 8$ m^3/t, with a maximum of 8.63 m^3/t, all located in abnormal coal seam and geological structure areas. The relationship between gas content occurrence and geological structure is shown in TABLE 1.

TABLE 1

The relationship between gas content and geological structure in the first mining area

Sampling location	Sampling elevation/m	Gas Content/ m^3/t	Geological conditions
11501 Transport Bottom Extraction Lane Y32-1 # Hole	–1055.2	8.3882	F11501-20 224°∠15°~30° H = 2.5 m±
11501 track bottom 11 # drilling site G11-2 # hole	–983.0	8.1728	FX23 210°∠60° H = 1.5 m
11502 Top Extraction Lane 20 # Drilling Site 150-8 # Hole	–1034.1	8.6324	The dip angle of the coal seam changes from –7° to –11° and then to –7°
11502 Top Extraction Lane 25 # Drilling Site 187-8 # Hole	–1049.9	8.098	32m away from the axis of the Shiwei syncline
11501 Bottom Transport 20 # Drilling Site Y20-1 # Hole	–1021.4	7.9211	FX30 243°∠50° H = 1.0 m±
11501 Bottom Transport 24 # Drilling Site Y24-1 # Hole	–1042.3	7.3202	F11501-5 23°∠30° H = 1.2 m±
11501 Bottom Transport Y28-1 # Hole	–1051.7	7.1295	Normal fault ∠60°, H = 0.2 m
11501 Bottom Transport Y28-2	–1051.7	7.1295	Normal fault ∠60°, H = 0.2 m
11501 track bottom 18 # drilling site G18-1 # hole	–1004.7	7.094	The dip angle of the coal seam changes from +6° to –4 °
11501 rail bottom 30 # drilling site G30-1 # hole	–1058.9	7.0159	8m away from the axis of the Shiwei syncline
11501 Transport Bottom Extraction Lane Y32-1 # Hole	–1051.5	7.1731	The coal thickness changed from 1.5 m to 1.3 m and then to 1.8 m

It can be seen from TABLE 2 that N_2: CO_2: CH_4 = 3.51%~68.87%: 1.29%~20.17%: 27.15%~94.13% in the natural gas composition of the coal seam 11-2. The CH_4 composition tested by only three boreholes is greater than 80%. The thickness of the tertiary ~Quaternary

loose layer of coal measure stratum of the mine is 340~600 m. After calculation, the depth of the gas weathering zone is 810~1070 m, and the buried depth of coal seam 11-2 is 960~1080 m. Therefore, most areas of coal seam 11-2 are located in the N2-CH_4 zone. According to the measured gas content during the development and mining of coal seam 11-2, the elevation of –923.8~–1059.4 m is selected, and a maximum value is selected from the elevation drop of every 10 m to construct the linear regression relationship between the gas content of coal seam and the buried depth of coal seam, as shown in Fig. 3.

TABLE 2

Gas content and composition test results of 11-2 coal seam in the first mining area during the geological prospecting period

Namber	The Natural composition of gas /%					Floor elevation /m	Gas content /m^3/t	Remarks
	N_2	CO_2	CH_4	C_2H_6	C_3H_8			
34-1	17.07	11.79	71.14			–957.84	49.54	Fourth mining area
34-2	30.62	7.02	61.52	0.69	0.15	–1017.87	3.15	
34-3	37.35	14.12	47.83	0.10	0.26	–1056.45	3.67	
34-4	3.51	6.34	87.33	1.97	0.44	–1057.92	9.79	
35-1	51.49	16.46	32.05			–1056.26	1.17	
35-2		3.79	94.13	1.84	1.05	–1015.29	12.21	
35-3	8.59	2.59	87.96	0.78	0.08	–1066.43	14.82	
36-1	15.25	6.48	78.27			–965.28	5.31	Fifth mining area
36-2	29.73	16.54	52.17	1.02		–1008.81	2.36	
36-3	53.88	8.09	38.03			–1045.70	4.63	
36-4	13.81	9.16	76.18	0.66	0.20	–1046.75	2.09	
37-4	45.77	3.20	50.61	0.33	0.09	–983.07	5.88	
38-1	30.48	41.16	27.56			–860.60	1.75	
38-2	52.68	20.17	27.15			–931.83	0	
38-4	68.87	1.29	29.84			–1067.09	0.8	

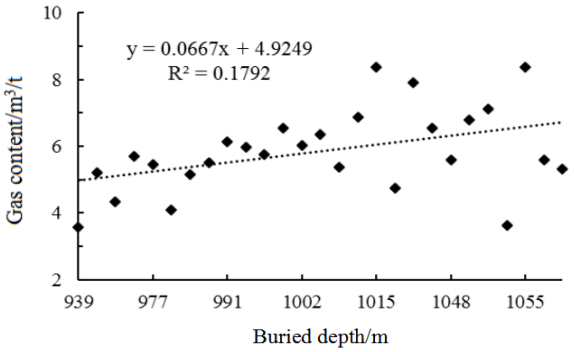

Fig. 3. The relationship between gas content and elevation of 11-2 coal seam in the first mining area

It can be seen from Fig. 3 that the gas content of coal seam 11-2 is 2.23~8.6324 m^3/t, with an average of 5.48 m^3/t. According to the fitting regression analysis, the correlation coefficient

between gas content and coal seam buried depth is only 0.1729. The law of gas content increasing with the increase of coal seam buried depth is not obvious, and the distribution of gas content is discrete. At the same time, through the statistical analysis of the measured gas content of coal seam 11-2, there are 4 groups with gas content $w \geq 8$ m^3/T, the maximum is 8.63 m^3/t, and they are all in the abnormal area of coal seam and geological structure area. 83% of the 18 groups with 7 m^3/T $\leq w <$ 8 m^3/ Tare in the abnormal area of coal seam and geological structure area, and the rest are less than 7 m^3/T. To sum up, the gas content generally increases with the increase of coal seam buried depth, but the law is not obvious, the gas occurrence is uneven, and the gas content is generally low compared with typical outburst coal seams.

2. Theoretical analysis on the feasibility of protective layer mining

2.1. Analysis of mining height and interlayer distance of protective layer

According to the detailed rules for the prevention and control of coal and gas outbursts, when the expansion deformation of the protected layer is greater than 3‰ [24], the mining of the protected layer can effectively protect the protected layer. When the buried depth of 11-2 Coal Seam in 11501 working face of Zhujixi mine is 960~1080 m, and the cutting width of the working face is 220 m, the minimum effective mining thickness of the protective layer is 0.9 m. The design mining thickness of the 11501 working face is 2 m, so the mining thickness of the protective layer meets the requirements. The maximum effective protection vertical distance between the protective layer and the protected layer can be determined according to formula (1):

$$S_X = S'_X \beta_1 \beta_2 \tag{1}$$

Where:

S'_X – Theoretical effective spacing of lower protective layer, m;
β_1 – Influence coefficient of protective layer mining, when $M \leq M_0$, $\beta_1 = M/M_0$, when $M > M_0$, $\beta_1 = 1$;
M – Mining thickness of protective layer, m;
M_0 – Minimum effective thickness of protective layer, m;
β_2 – Proportion coefficient of hard rock (fine sandstone, siltstone, etc.) in rock stratum, Percentage of hard rock in rock stratum η express, when $\eta \geq 50\%$, $\beta_2 = 1\text{-}0.4\eta/100$, when $\eta < 50\%$, $\beta_2 = 1$.

The mining height of the 11501 working faces is 2 m, the cutting width is L = 220 m, and the mining depth is h = 983~1083 m, which is determined by the detailed rules for the prevention and control of coal and gas outbursts, S'_X = 114~122 m, $\beta_1 = 1$, $\beta_2 = 1$, According to formula (1): S_X = 114~122 m. The maximum interval between the 11-2 Coal Seam and the overlying 13-1 coal seam in the 11501 working faces is 73 m, which is less than the maximum protection vertical distance. Therefore, the 11-2 Coal seam can be used as the lower protection layer of 13-1 coal seam.

At the same time, according to the detailed rules for the prevention and control of coal and gas outbursts, the resources of the upper adjacent layer shall not be damaged when mining the lower protective layer, and the minimum interlayer distance between the protective layer and the protected layer can be determined according to formula (2):

$$\text{When } \alpha < 60°,\ H = K\cos\alpha \tag{2}$$

Where:

H – Minimum allowable layer spacing,m;
A – Coal seam dip, 5°;
K – Roof management coefficient. When the roof of the goaf is managed by the caving method, $K = 10$.

According to the occurrence conditions of a coal seam in 11501 working face, $H = 9.96$ M can be calculated from formula (2), which is far less than the spacing between the two coal seams. Therefore, coal seam 11-2 can be used as the lower protective layer of coal seam 13-1.

2.2. Theoretical calculation of "three zones" height of 11-2 Coal Seam

Coal seam mining is easy to cause the movement, deformation, and damage of surrounding rock in the goaf. Under the interaction of self-weight stress and surrounding rock, the roof rock stratum(they are rather caving rocks without any additive) produces a violent instability and rebalancing process, forming the "upper three zones" above the goaf as shown in Fig. 4. Generally, it will not damage the integrity of the adjacent coal seam roof in the high fracture zone and low bending subsidence zone, Its mining will not be affected, but due to the pressure relief of the coal seam, the permeability becomes stronger, which is beneficial to gas drainage and can eliminate or reduce the outburst risk.

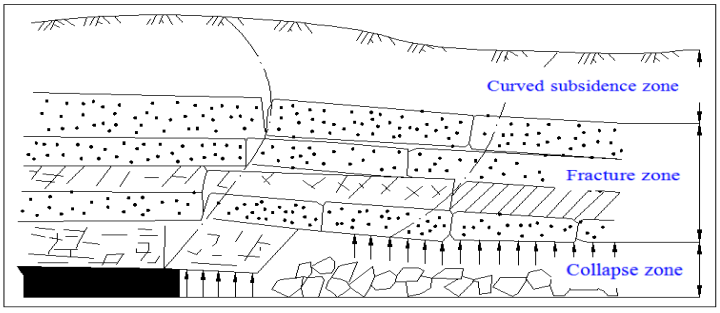

Fig. 4. Zonation model of "upper three zones"

Base on the various lithologies of the coal seam overburden, the heights of the caving zone (H_m) and fracture zone (H_L) can be calculated. According to the occurrence conditions of coal strata in the test area, the coal seams 11-2 and 13-1 are mainly siltstone, fine sandstone, and mudstone, with unidirectional compressive strength of 55.99 MPa (45.8~79.6 Mpa), 78.06 MPa

(60.8~119.9 Mpa) and 37.08 Mpa (22~69.3 Mpa) respectively. The interlayer lithology is mainly hard rock, and the calculation formula of collapse zone height is:

$$H_m = \frac{100\sum M}{2.1\sum M + 16} \pm 2.5 \tag{3}$$

The average thickness of coal seam 11-2 is 1.6 m. The mining technology of full-height mining at one time is adopted. After calculation, the height of the collapse zone of the coal seam 11-2 is HM = 6.6~11.6 m.

The calculation formula for fracture zone height is:

$$H_L = \frac{100\sum M}{1.2\sum M + 2.0} \pm 8.9 \tag{4}$$

After calculation, the height of the fracture zone of the coal seam 11-2 is H_L = 34.4~52.2 m.

After the mining of the 11-2 Coal Seam, the protected 13-1 coal seam is in the high fracture zone or low bending subsidence zone. The continuity of the 13-1 coal seam will not cause a destructive impact, which can significantly increase the permeability of the 11-2 Coal seam. To sum up, through the analysis of the reasonable layer spacing and the development height of the collapse zone and fracture zone of 11-2 Coal Seam as a protective layer, it can be seen that 11-2 Coal seam can be used as the protective layer under 13-1 coal seam.

3. Outburst prevention technology in the underground pumping area

When the protective layer is mined, under the action of self-weight and overburden pressure, the overlying coal layer in the goaf will move to the goaf, producing bedding and through cracks, which greatly increases the permeability of the coal layer and obtains a good channel for the migration of coal seam gas. For underground coal and gas outburst prevention and control, protective layer mining is the most economical and effective regional outburst prevention measure. Therefore, for determining the pressure relief range and protection effect of the protected layer, it is of great significance to study the vertical stress distribution law and deformation characteristics of the roof and floor strata after the mining of the protected layer. Due to the complexity of the mining effect of coal seam roof and floor, if we only use the theories of elastic-plastic mechanics and material mechanics to study, we can not accurately calculate the stress distribution in the overlying rock after the mining of the protective layer. Under the background of the rapid development of the computer industry, the numerical simulation method makes modeling and transformation of the physical field more convenient and fast. Mining models under different conditions can be established according to actual needs, and their unique advantages can be demonstrated at the same time.

In this paper, the combination of numerical simulation and field investigation is used to study the pressure relief protection effect of the 11-2 Coal Seam on the overlying 13-1 coal seam after mining.

3.1. Establishment of numerical model

According to the occurrence of 11501 working face and overlying coal strata of 11-2 Coal Seam, FLAC3D software is used to establish a model with a dip length of 320 m (*x* direction), a strike length of 380 m (*Y* direction) and a height of 190 m (z-direction). The mining thickness of the 11501 working face is 2 m, the average thickness of the 13-1 coal seam is 3.8 m, and the average interval between the two coal seams is 70 m. To reduce the influence of coal seam mining on the whole model, 80 m coal pillars are reserved along the strike and inclination of the coal seam. The upper boundary of the model is free, and the bottom boundary and left and right boundaries adopt zero displacement boundary because the thickness of the overlying strata of the simulated mining coal seam has a certain range, the lateral pressure coefficient is 1.0, and the horizontal stress is applied to the front, back, left and right of the model. The goaf is modeled using a rectangular structure, and the strength and deformation parameters are based on the strength and deformation parameters of 11 coal in TABLE 2. The numerical simulation model is shown in Fig. 5, and the material physical and mechanical parameters of the model are shown in TABLE 3.

The Mohr-Coulomb plastic constitutive model and Mohr-Coulomb yield criterion are adopted for calculation, namely:

$$f_s = \sigma_1 - \frac{\sigma_3(1+\sin\varphi)}{1-\sin\varphi} + 2c\sqrt{\frac{1+\sin\varphi}{1-\sin\varphi}} \tag{5}$$

$$f_t = \sigma_3 - \sigma_t \tag{6}$$

Where:

σ_1, σ_3 – Maximum and minimum principal stresses, MPa;
c – The cohesion of rock stratum, MPa;
φ – Is the internal friction angle of rock stratum,°;
Σ_t – Tensile strength of rock stratum, MPa; when $f_s = 0$, Shear failure of rock mass, when $f_t = 0$,Tensile failure of rock mass.

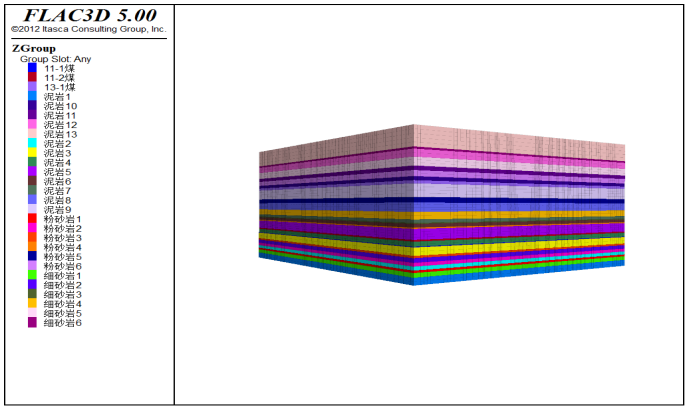

Fig. 5. Numerical model diagram

TABLE 3

Table of physical and mechanical parameters of numerical simulation strata

Lithology	Bulk density /kg/m^3	Bulk modulus /GPa	Shear modulus /GPa	Tensile strength /MPa	Cohesion /MPa	Internal friction angle/°	Bulk modulus /GPa
mudstone	2461	6.08	3.47	1.0	1.2	30	6.08
fine sandstone	2873	20.01	13.52	2.9	3.2	42	20.01
Siltstone	2460	10.83	8.13	2.6	2.75	38	10.83
mudstone	2461	6.08	3.47	1.0	1.2	30	6.08
13-1 coal	1350	4.91	2.01	0.9	1.25	32	4.91
mudstone	2461	6.08	3.47	1.0	1.2	30	6.08
Siltstone	2460	10.83	8.13	2.6	2.75	38	10.83
mudstone	2461	6.08	3.47	1.0	1.2	30	6.08
fine sandstone	2873	20.01	13.52	2.9	3.2	42	20.01
mudstone	2461	6.08	3.47	1.0	1.2	30	6.08
11-2 coal	1420	4.91	2.01	0.9	1.25	32	4.91
mudstone	2461	6.08	3.47	1.0	1.2	30	6.08
Siltstone	2460	10.83	8.13	2.6	2.75	38	10.83
mudstone	2461	6.08	3.47	1.0	1.2	30	6.08
Siltstone	2460	10.83	8.13	2.6	2.75	38	10.83

3.2. Analysis of numerical simulation results

3.2.1. Analysis of vertical stress variation of overlying 13-1 coal seam after mining 11-2 Coal Seam

In this simulation, the width of the 11501 working face is 220 m, and the mining length is 160 m. The model is mined along the tendency, and the excavation step is 20 m. Due to the limitation of the FLAC3D post-processing project, Tecplot software is used for graphic processing. The vertical stress contour at the positions of 20 m, 40 m, 80 m, 100 m, 120 m, 140 m, and 160 m, y = 190 m in the working face is shown in Fig. 6.

According to the vertical stress distribution along the dip direction at different mining distances of the working face of the protective layer in Fig. 6, when the working face is mined for 20 m, the vertical stress of the coal strata around the goaf does not change significantly, only the stress of the roof and floor strata decreases significantly within a certain range. The stress of the roof and floor strata decreases the most in the middle of the goaf, and the vertical stress is distributed in an arch shape, the degree of reduction decreases gradually with the increase of the distance from the goaf. There is obvious stress concentration behind and in front of the cutting hole of the working face, and the stress distribution is symmetrically distributed along the middle of the mining length. As shown in Fig. 6(b), after 40 m of working face mining, the vertical stress of the coal layer overlying the goaf at the same layer is significantly reduced compared with that at 20 m of mining, and the reduction range of vertical stress in the horizontal direction gradually increases, indicating that the pressure relief degree of the coal layer overlying the goaf gradually increases, while the vertical stress at the arch foot gradually increases, but with the increasing range of goaf, Under the influence of self-weight and other effects, the roof rock stratum gradu-

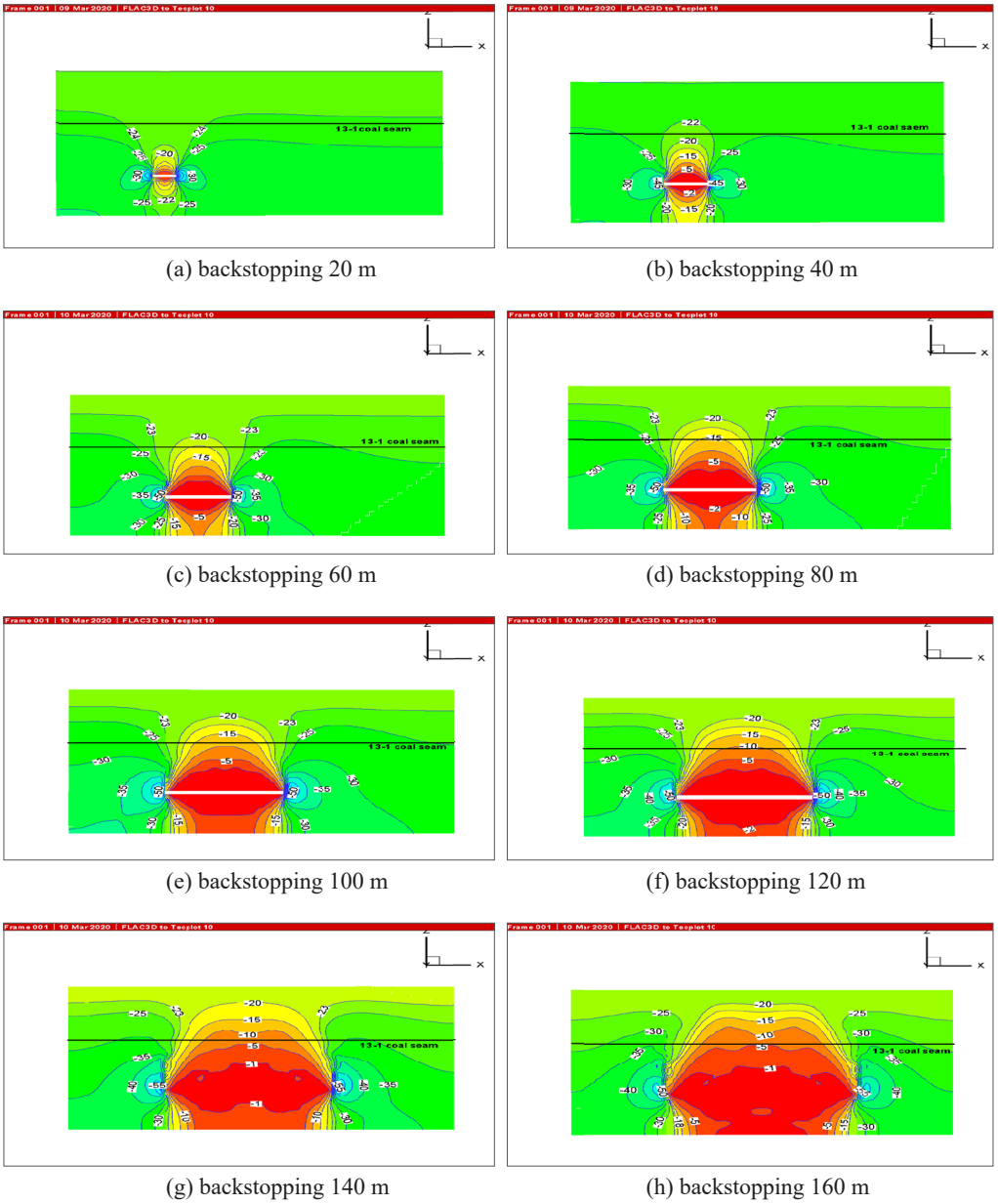

(a) backstopping 20 m (b) backstopping 40 m

(c) backstopping 60 m (d) backstopping 80 m

(e) backstopping 100 m (f) backstopping 120 m

(g) backstopping 140 m (h) backstopping 160 m

Fig. 6. Contour map of vertical stress along the inclined direction at different distances in 11501 working face

ally moves to the goaf, the caving gangue fills the goaf, compacts it continuously, and the vertical stress recovers. As shown in Fig. 6(d), after 80 m mining of the working face, the vertical stress of the coal stratum overlying the goaf changes slightly, and the vertical stress contour changes from arch distribution to camel distribution. As shown in Fig. 6(g), after the working face is mined

for 140 m, the vertical stress of the coal stratum in the vertical direction will no longer increase with the increase of the mining length of the working face, and the range of the vertical stress contour in the horizontal direction will gradually increase with the increase of the mining length.

To study the dynamic change process of the stress of coal seam 13-1 when coal seam 11-2 is pushed for different distances, observation points are arranged on the floor of coal seam 13-1, the stress data of each observation point are recorded, and the change curve of the vertical stress of the protected layer with the mining of the protected layer is obtained, as shown in Fig. 7.

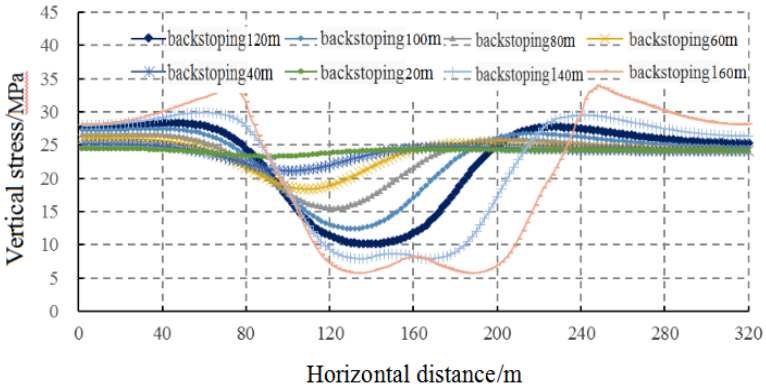

Fig. 7. The vertical stress change trend diagram of the 13-1 coal seam along the inclined direction when the 11501 working face is mined at different distances

It can be seen from Fig. 7 that when working face 11501 is stopped for 20 m, the minimum vertical stress of coal seam 13-1 overlying the goaf is 23.25 MPa, which is 24.13 MPa relative to the original rock stress, and the stress reduction rate is 3.64%. The stress concentration in the front of the work and at the cutting hole is not obvious, indicating that coal seam 13-1 is less affected by the mining of underlying coal seam 11-2 at this time; With the increase of the mining length of the working face, the vertical stress of the overlying 13-1 coal seam gradually decreases and the pressure relief range gradually increases. For example, when the working face is mining 40 m, 60 m, 80 m, 100 m, 120 m, 140 m and 160 m, the vertical stress of the 13-1 coal seam directly above the middle of the goaf is 21.16 MPa, 18.41 MPa, 15.55 MPa, 12.43 MPa, 10.15 MPa, 8.64 MPa and 8.06 MPa respectively, and the stress reduction rates are 12.31% and 23.70% respectively 35.56%, 48.48%, 57.94%, 64.19% and 66.59%. The decline range of vertical stress first increases then decreases and finally tends to be stable, indicating that the pressure relief degree of coal seam 13-1 gradually increases with the increase of working face distance. After mining to 140 m, the goaf should be continuously filled and compacted, resulting in stress recovery, and the pressure relief degree of coal seam 13-1 tends to be stable, The pressure relief range increases with the increase of the working face length.

According to the numerical simulation results, Tecplot software is used to obtain the vertical stress isolines at x = 90 m, 100 m, 110 m, 120 m, 130 m, 140 m, 150 m and 160 m at different mining distances in the strike direction, as shown in Fig. 8.

It can be seen from Fig. 8 that under the occurrence condition of a near horizontal coal seam, the vertical stress distribution and variation law of overlying coal strata in goaf is the same with

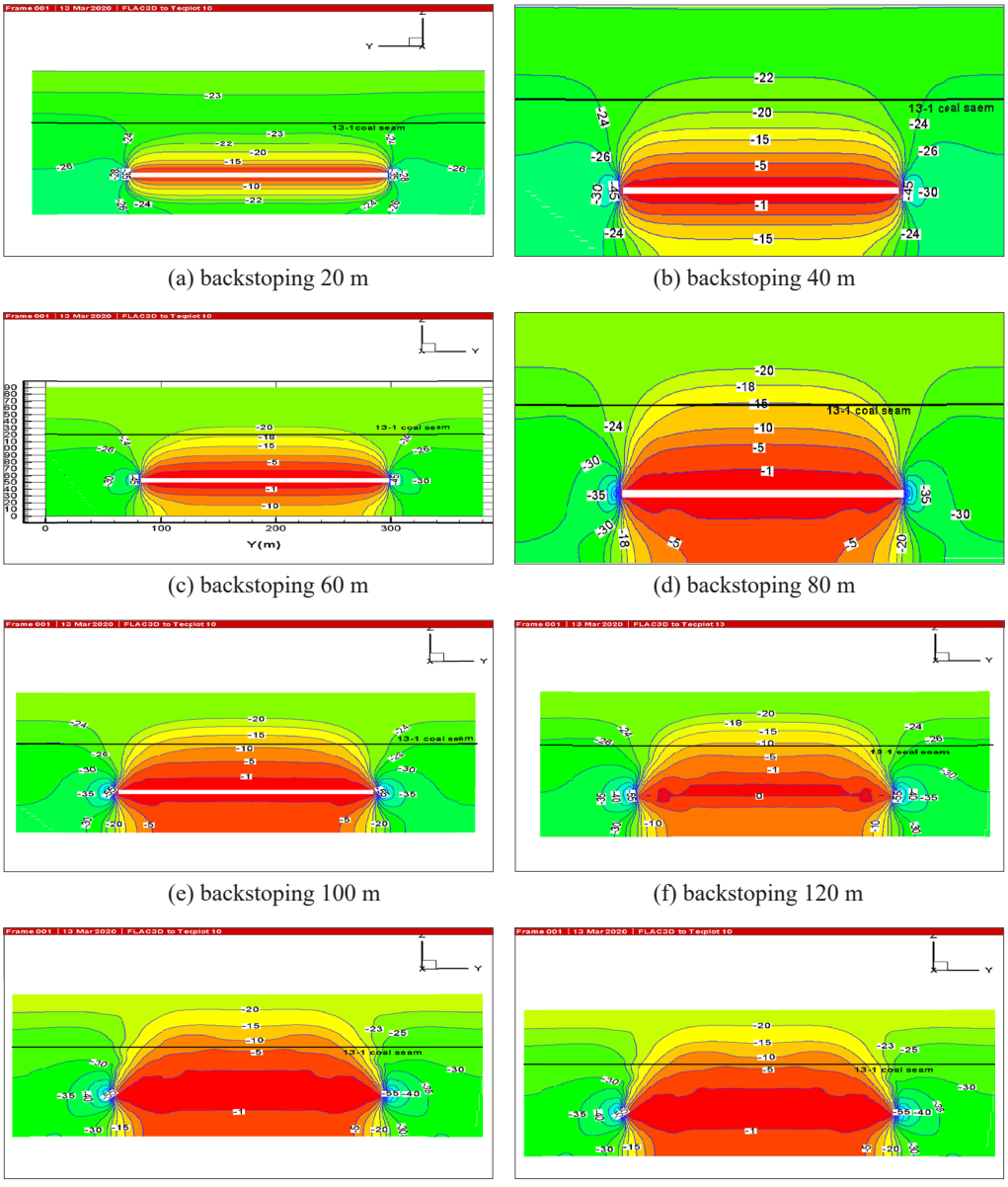

(a) backstoping 20 m (b) backstoping 40 m

(c) backstoping 60 m (d) backstoping 80 m

(e) backstoping 100 m (f) backstoping 120 m

(g) backstoping 140 m (h) backstoping 16 m

Fig. 8. Contour map of vertical stress along strike direction at different distances in 11501 working face

the increase of mining length of working face in the strike and dip direction of the coal seam. The research shows that when the stress reduction rate of the protected layer is more than 50%, the coal seam is fully relieved, and the air permeability is enhanced. The extraction of coal seam 11-2 in the protected layer effectively relieves pressure on coal seam 13-1 in the protected layer.

3.2.2. Analysis of vertical displacement change of overlying 13-1 coal seam in 11-2 Coal Seam Mining

The vertical displacement contour at the positions of 20 m, 40 m, 80 m, 100 m, 120 m, 140 m and 160 m, y = 190 m, is shown in Fig. 9.

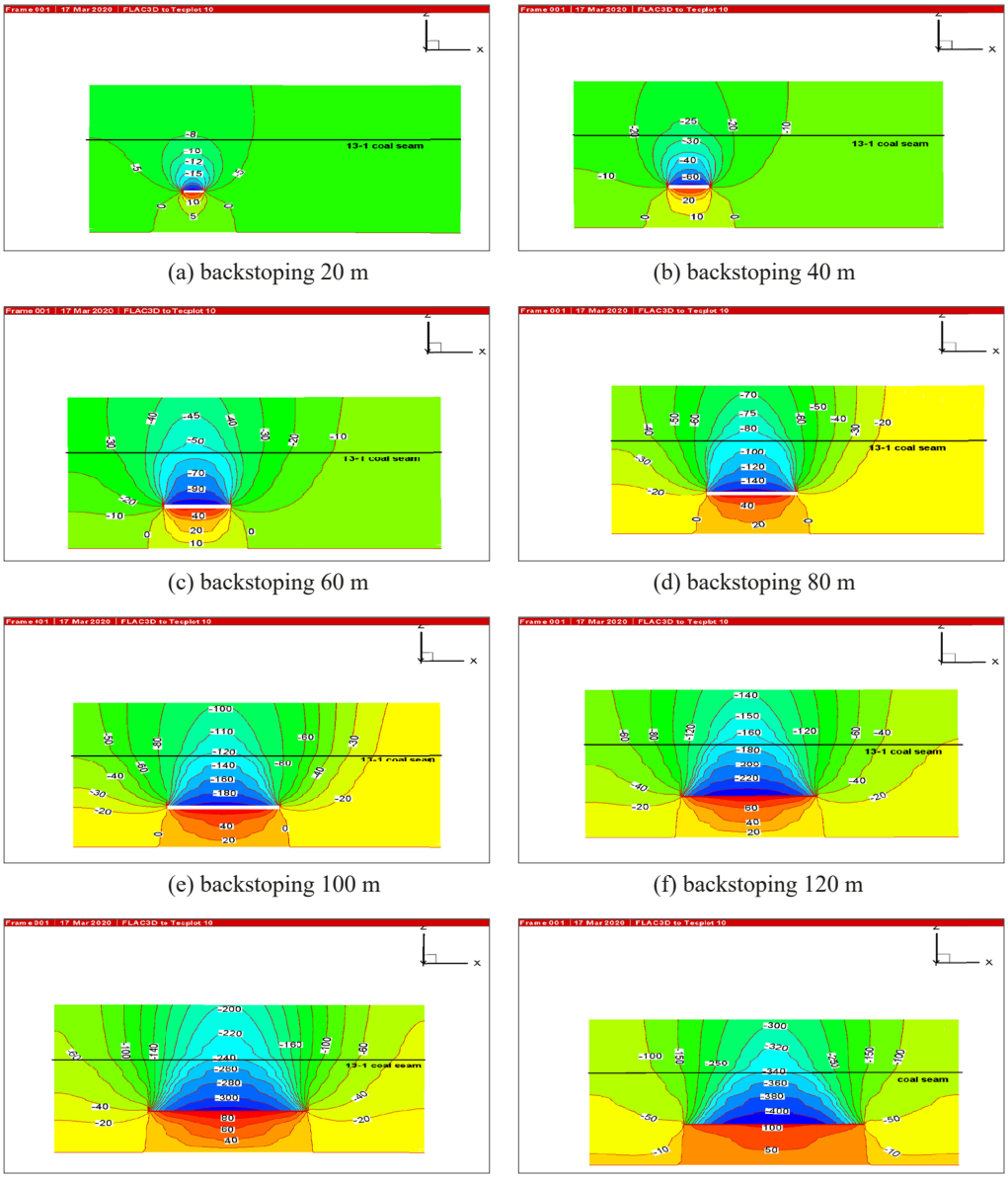

(a) backstoping 20 m (b) backstoping 40 m

(c) backstoping 60 m (d) backstoping 80 m

(e) backstoping 100 m (f) backstoping 120 m

(g) backstoping 140 m (h) backstoping 160 m

Fig. 9. Contour map of vertical displacement along strike direction at different distances of 11501

It can be seen from Fig. 9 that after the mining of the working face, the original rock stress balance state of the surrounding rock strata is broken, and the coal seam roof and floor move towards the goaf under the action of the initial in-situ stress field. With the increase of the mining distance of the working face, the displacement of the coal strata in the same layer above or below the goaf gradually increases. When the 11-2 coal seam is mined for 40 meters, the damage-affected area above reaches 60 meters and has not yet affected the overlying 13-1 coal seam. When the 11-2 coal seam is mined for more than 60 meters, the damage affected area above reaches 90 meters and has already exceeded the position of the 13-1 coal seam. The deformation of the overlying 13-1 coal seam begins to change, The horizontal square lines are symmetrically distributed along the middle of the goaf. Under the conditions of different mining lengths, the movement and deformation laws of coal and rock strata are the same.

To investigate the expansion deformation of the overlying 13-1 coal seam at various mining distances from the 11501 working face of the 11-2 coal seam, measurement points are arranged along the incline at both the top and bottom of the 13-1 coal seam. The displacement of the top and bottom of the 13-1 coal seam during the mining of the 11-2 coal seam is recorded using Tecplot software. After calculation, the variation trend of the displacement of the top and floor of the 13-1 coal seam with the mining length of the working face is shown in Fig. 10.

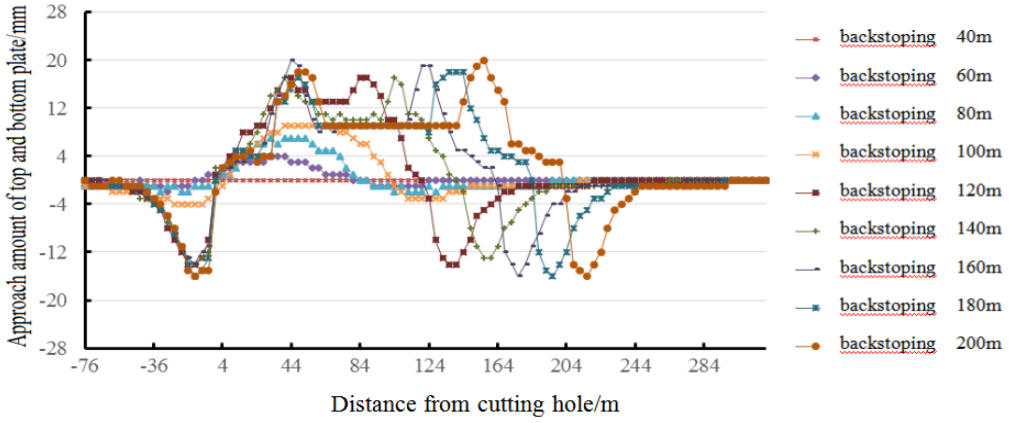

Fig. 10. Change trend of 13-1 coal seam roof and floor approaching amount at different distances in 11501 working face

When the 11501 working face is advanced to 40 m, there is no expansion trend in 13-1 coal seam, and the expansion curve is displayed as a straight line, indicating that the mining of 11-2 Coal Seam has no impact on the deformation of overlying 13-1 coal seam; When 11501 working face advances to 60 m, the deformation of overlying 13-1 coal seam begins to change, the area and degree of expansion begin to change are still small, and the maximum expansion area appears directly above the goaf.

In conclusion, with the increase of the mining length of the working face of coal seam 11-2, the stress of the overlying coal seam 13-1 in the goaf decreases greatly, and the expansion deformation rate of the coal seam is greater than 3‰, which is 4.25‰, indicating that the mining of coal seam 11-2 is effective in the pressure relief protection of overlying coal seam 13-1.

3.3. Field practice analysis

Based on the on-site construction conditions of 11501 roof roadway, 100 m ahead of the working face of the protective layer was determined, a deep base point displacement meter was installed, and the relative displacement of the roof and floor of the protected coal seam during the mining process of the working face of the protective layer was continuously observed. The variation trend of roof and floor approaching the amount of coal seam 13-1 before and after mining of coal seam 11-2 of the protective layer is shown in Fig. 11.

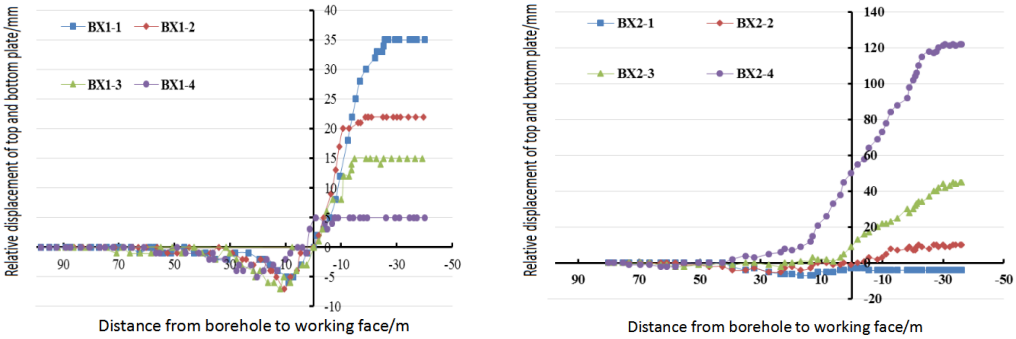

(a) Tendency direction (b) Strike direction

Fig. 11. The 13-1 coal seam roof and floor displacement changes with the advancement of the protective layer

Through the test of the movement of the roof and floor of coal seam 13-1 during the mining of coal seam 11-2 of the protective layer, according to the calculation formula of the expansion deformation of coal seam, the maximum expansion deformation of coal seam 13-1 at different positions after the mining of coal seam 11-2 is shown in TABLE 4.

TABLE 4

11-2 Different drill holes after coal seam 13-1 maximum swelling deformation of coal seam

Number	Relative displacement /mm	Coal hole section length /m	Expansion deformation /‰	Remarks
BX1-1	35	4.8	7.29	Tendency direction
BX1-2	22	4.3	5.12	
BX1-3	15	5.2	2.88	
BX1-4	5	5.0	1.00	
BX2-1	–4	7.7	–0.52	Strike direction
BX2-2	10	6.1	1.14	
BX2-3	45	5.0	3.89	
BX2-4	122	5.2	23.46	

TABLE 4 shows that the relative deformation of coal seams corresponding to borehole bx1-1 and bx1-2 in the dip direction is greater than 3‰, which is within the effective pressure relief range; According to the relative deformation of coal seams measured by bx1-1, bx1-2, bx1-3 and

bx1-4 boreholes, the pressure relief angle in the dip direction is 63.70, the pressure relief angle in the strike direction is 80.8, and the pressure relief line corresponds to the stoping line of the working face of the protective layer with an internal error of 37.20 m.

3.4. Effect of outburst prevention technology of combined pumping up and down the well

The prevention and control of coal and gas outbursts is related to coal mining. The premise of coal mine development and mining is to achieve effective outburst prevention and up-to-standard drainage, and also pay attention to the coordination and unity between gas drainage and mining production. For the long-distance coal seam group with flat ground, both surface wells and underground boreholes can carry out gas pre-drainage and pressure relief drainage, but economic and efficient outburst prevention and effective well up and down combined drainage method with standard drainage should be constructed.

3.4.1. Analysis of gas control effect of working face in protective layer

During the mining period of 11501 working face, the gas in this coal seam is mainly extracted by drilling along the layer, burying pipes in the goaf and high-level drilling in the roof roadway, and the pressure relief gas in the adjacent layer is extracted by the combination of through layer drilling and surface drilling [24-25]. To investigate the gas control effect of the above measures on the working face, the data during the period of maximum gas concentration in the return airflow during mining are selected for statistical analysis, and the variation curve of gas concentration with time is drawn, as shown in Fig. 12.

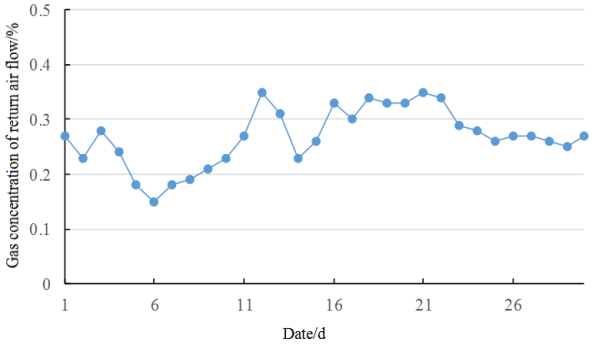

Fig. 12. Variation law of gas concentration with time in the return airflow of 11501 working face

It can be seen from Fig. 11 that during this period, the gas concentration in the return airflow is below 0.35%, and a large amount of gas in the working face is pumped so that the gas concentration in the return airflow is within the normal range and relatively stable. There is no gas overrun problem during the mining of the working face to ensure the safe mining of the working face. Therefore, The measures taken during mining in the working face have achieved a good gas control effect.

3.4.2. Analysis of gas drainage effect in protective layer working face

During the mining period of the working face, the method of mining and pumping while drilling along the stratum, burying pipes in the goaf, high-level drilling on the roof and surface drilling is adopted to control gas. It can be seen from Fig. 13 and Fig. 14 that the gas concentration and flow rate of bedding borehole drainage remain unchanged, the drainage concentration is less than 1.5%, and the flow rate is less than 1 m^3/min; The concentration of gas extraction by buried pipes in goaf is about 2%~5%, the net flow of gas extraction is 1~3 m^3/min, the concentration of gas extraction by high-level boreholes in roof roadway is 2%~10%, and the net flow of gas extraction is 1~3 m^3/min. The concentration and flow of gas extraction by buried pipes in goaf and high-level boreholes in the roof fluctuate significantly compared with that by bedding holes, which is mainly caused by different footage of the working face and uneven gas storage in the working face.

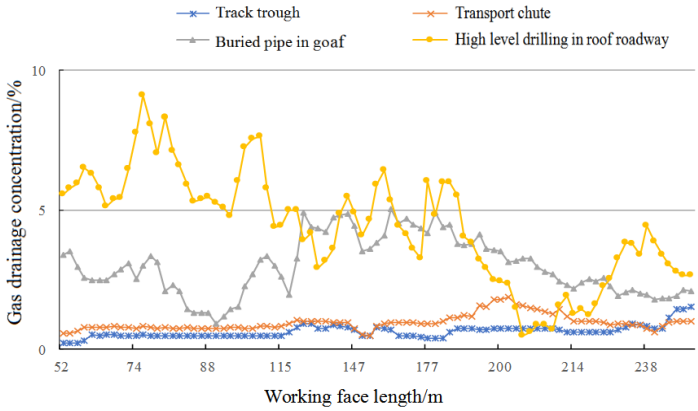

Fig. 13. Variation law of gas drainage concentration with working face advancing

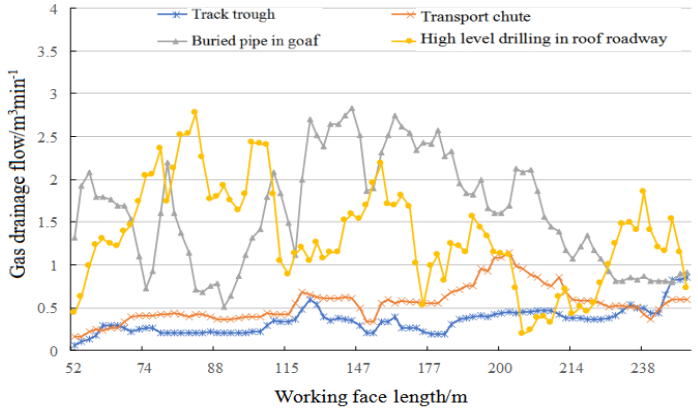

Fig. 14. Variation law of gas drainage flow with advancing of working face

4. Conclusion

Taking the occurrence of long-distance outburst coal seams in the Zhujixi coal mine as the research background, using the combination of theoretical analysis, calculation, numerical simulation and field practice, this paper analyzes the gas occurrence characteristics of 11-2 Coal Seam and the feasibility of 11-2 Coal Seam as the lower protective layer, and studies and determines the pressure relief protection range of 11-2 Coal Seam Mining to the overlying 13-1 coal seam; This paper puts forward the regional outburst prevention technology of underground penetrating and bedding borehole pre drainage for the protective layer and the regional outburst prevention technology of pre drainage combined with the mining surface and underground of the protected layer. The conclusions are as follows:

(1) Coal seam 11-2 has uneven gas occurrence and poor regularity. There are only high gas areas in some parts, which are greatly affected by the geological structure and slate properties of the coal seam top and bottom. Coal seam 11-2 is a stress-dominated briquette and gas outburst coal seam. The height of the "upper three zones" during the mining of the 11-2 Coal seam is theoretically calculated, and the feasibility of protective layer mining is demonstrated through numerical simulation, which provides a basis for the layout of the working face of the protected layer.

(2) Adopts the regional outburst prevention mode of combined pumping up and down the well, that is, 11-2 Coal with low outburst risk is selected as the protective layer for mining first, 13-1 coal is protected above, and the gas of the protected layer is pumped at the same time. 11-2 Coal adopts the gas control mode of "one side with three lanes (one side with five lanes in the first mining face) + surface drilling", to realize multi-purpose, joint treatment and continuous mining of one lane. The tunnelling working face adopts cross-layer drilling and pre-pumping, and the coal mining working face adopts the comprehensive outburst prevention measures of bedding drilling and pre-pumping area. During the mining period, the ground drilling and top drainage roadway are used to extract the pressure relief gas of 13-1 coal.

(3) Using the technology of up-down combined pumping area, the underground excavation and mining face, the gas concentration of return airflow, the measured residual gas content and residual gas pressure, and the prediction indexes have not exceeded the standard, and there has been no dynamic phenomenon. In the application of up-down combined pumping area outburst prevention technology in the Zhujixi mine, the proportion of up-down pumping is 56.7%, and the proportion of down-hole pumping is 43.3%, Both are indispensable.

Acknowledgments

This work was supported by the coal Mine Safety Mining Equipment innovation center of Anhui Province (No.CMSMEICAP2023005) and the national natural Sciencefoundation of china (no. 52174103)

Reference

[1] S.H.W. Vick, P. Greenfield, K.L. Pinetown, N. Sherwood, S. Gong, S.G. Tetu, D.J. Midgley, I.T. Paulsen, Succession Patterns and Physical Niche Partitioning in Microbial Communities from Subsurface Coal Seams. Science **12**, 152-167 (2019). DOI: https://doi.org/10.1016/j.isci.2019.01.011

[2] H.P. Hou, Z.Y. Ding, S.L. Zhang, S.C. Guo, Y.J. Yang, Z.X. Chen, J.X. Mi, X. Wang, Spatial estimate of ecological and environmental damage in an underground coal mining area on the Loess Plateau: Implications for planning restoration interventions. Journal of Cleaner Production **287**, 125061 (2021). DOI: https://doi.org/10.1016/j.jclepro.2020.125061

[3] Y. Hao, Z.Y. Zhang, H. Liao, Y.M. Wei, China's farewell to coal: A forecast of coal consumption through 2020. Energy Policy **86**, 444-455 (2015). DOI: https://doi.org/10.1016/j.enpol.2015.07.023.

[4] X.Z. Chen, S. Xue, L. Yuan, Coal seam drainage enhancement using borehole presplitting basting technology – A case study in Huainan. International Journal of Mining Science and Technology **27**, 771-775 (2017). DOI: https://doi.org/10.1016/j.ijmst.2017.07.015

[5] C. Zhang, F.T. Wang, Q.S. Bai, Underground space utilization of coalmines in China: A review of underground water reservoir construction. Tunnelling and Underground Space Technology **107**, 103657 (2021). DOI: https://doi.org/10.1016/j.tust.2020.103657

[6] X.Y.P.G. Ranjith, F. Dang, Analysis of Deformation, Permeability and Energy Evolution Characteristics of Coal Mass Around Borehole After Excavation. Nat. Resour. Res. **29**, 3159–3177 (2020). DOI: https://doi.org/10.1007/s11053-020-09644-0

[7] D. Sha, B.F. Pan, Y.R. Sun, A novel raw material for geopolymers: Coal-based synthetic natural gas slag. Journal of Cleaner Production **262**, 121238 (2020). DOI: https://doi.org/10.1016/j.jclepro.2020.121238

[8] X.G. Niu, D.D. Pang, H.H. Liu, et al., Gas Extraction Mechanism and Effect of Ultra-High-Pressure Hydraulic Slotting Technology: a Case Study in Renlou Coal Mine. Nat. Resour. Res. **32**, 321-339 (2023). DOI: https://doi.org/10.1007/s11053-022-10131-x

[9] B.Y. Jiang, B. Ji, L. Yuan, C.F.Yu, W.H. Tao, Y. Zhou, H.Y. Wang, X.H. Wang, M.L. Liao, Experimental and molecular dynamics simulation study of the ionic liquids' chain-length on wetting of bituminous coal. Energy **283** 0360-5442 (2023). DOI: https://doi.org/10.1016/j.energy.2023.128507

[10] H. Lu, Y.P. Cheng, L.Yuan, P. Chu, S.W. Wu, H. Wang, C.X. Zhao, L.Wang, Efficient-safe gas extraction in the superimposed stress strong-outburst risk area: Application of a new hydraulic cavity technology. Geoenergy Science and Engineering **240**, 2949-8910 (2024). DOI: https://doi.org/10.1016/j.geoen.2024.213076

[11] C. Xiao, L. Tian, Y.K. Yang, Y.Y. Zhang, D.H. Gu, S. Chen, Comprehensive application of semi-analytical PTA and RTA to quantitatively determine abandonment pressure for CO_2 storage in depleted shale gas reservoirs. Journal of Petroleum Science and Engineering **146**, 813-831 (2016). DOI: https://doi.org/10.1016/j.petrol.2016.07021

[12] Z.Q. Yin, Z.Y. Chen, J.C. Chang, Z.X. Hu, H.F. Ma, R.M. Feng, Crack Initiation Characteristics of Gas-Containing Coal under Gas Pressures. Geofluids 5387907 (2019). DOI: https://doi.org/10.1155/2019/5387907

[13] Y.W. Liu, Y. Du, Z.Q. Li, F.J. Zhao, W.Q. Zuo, J.P. Wei, H. Mitri, A rapid and accurate direct measurement method of underground coal seam gas content based on dynamic diffusion theory. International Journal of Mining Science and Technology **30** (6),799-810 (2020). DOI: https://doi.org/10.1016/j.ijmst.2020.07.004

[14] G.W. Dong, Y.H. Zou, A Novel Method for Selecting Protective Seam against Coal and Gas Outburst: A Case Study of Wangjiazhai Coal Mine in China. Sustainability **9** (6), 1015 (2017). DOI: https://doi.org/10.3390/su9061015

[15] G.H. Ni, K. Dong, S. Li, Q. Sun, Gas desorption characteristics effected by the pulsating hydraulic fracturing in coal. Fuel **236**, 190-200 (2019). DOI: https://doi.org/10.1016/j.fuel.2018.09.005

[16] C.A. Aylor, J.D. Sugar, D.B. Robinson, et al., Using In Situ TEM Helium Implantation and Annealing to Study Cavity Nucleation and Growth. JOM. **72**, 2032-2041 (2020). DOI: https://doi.org/10.1007/s11837-020-04117-4

[17] Y.P. He, W.Y. Lv, Z.Y. Fang, Li. Ma, C.K. Cong, The basic characteristics of paste backfill materials based on highly active mineral admixtures: Part I. Preliminary study on flow, mechanics, hydration, and microscopic properties. Process Safety and Environmental Protection **187**, 1366-1377 (2024). DOI: https://doi.org/10.1016/j.psep.2024.05.056.

[18] C.G. Lu, S.A. Zhang, D. Xue, F.C. Xiao, Liu, Improved estimation of coalbed methane content using the revised estimate of depth and CatBoost algorithm: A case study from southern Sichuan Basin. China. Computers & Geosciences **158**, 104973 (2022). DOI: https://doi.org/10.1016/j.cageo.2021.104973

[19] B.F. Gu, Y.L. Wu, Research and Application of Hydraulic Punching Pressure Relief Antireflection Mechanism in Deep "Three-Soft" Outburst Coal Seam. Shock and Vibration 7241538 (2021). DOI: https://doi.org/10.1155/2021/7241538

[20] L.S.Yuan, F.J. Zhou, M.H. Li, B. Wang, J.W. Bai, Experimental and numerical investigation on particle diverters transport during hydraulic fracturing. Journal of Natural Gas Science and Engineering **96**, 104290 (2021). DOI: https://doi.org/10.1016/j.jngse.2021.104290

[21] D.D. Yang, Y.J. Chen, J. Tang, X.W. Li, C.L. Jiang, C.J. Wang, C.J. Zhang, Experimental research into the relationship between initial gas release and coal-gas outbursts. Journal of Natural Gas Science and Engineering **50**, 157-165 (2018). DOI: https://doi.org/10.1016/j.jngse.2017.12.015

[22] B.Y. Jiang, Y. Zhao, B.Q. Lin, T. Liu, Effect of faults on the pore structure of coal and its resultant change on gas emission. Journal of Petroleum Science and Engineering **195**, 107919 (2020). DOI: https://doi.org/10.1016/j.petrol.2020.107919

[23] X.S. Zhao, H.T. Sun, J. Cao, et al., Applications of online integrated system for coal and gas outburst prediction: A case study of Xinjing Mine in Shanxi, China. Energy Science and Technology **8** (6), 1980-1996 (2020). DOI: https://doi.org/10.1002/ese3.642

[24] M. Wierzbicki, N. Skoczylas, The outburst risk as a function of the methane capacity and firmness of a coal seam. Archives of Mining Sciences **59** (4),1023-1031 (2014). DOI: https://doi.org/10.2478/amsc-2014-0070

[25] N. Skoczylas. M., Wierzbicki, Evaluation and management of the gas and rock outburst hazard in the light of international legal regulations. Archives of Mining Sciences **59** (4), 1119-1129 (2014). DOI: https://doi.org/10.2478/amsc-2014-0078